Journal of Nuclear Medicine, published on June 14, 2018 as doi:10.2967/jnumed.118.207811

Spatial normalization of ^{18}F-flutemetamol PET images utilizing an adaptive principal components template

Johan Lilja[1,2,*], Antoine Leuzy[3], Konstantinos Chiotis[3], Irina Savitcheva[4], Jens Sörensen[1], Agneta Nordberg[3,5]

[1]Department of Surgical Sciences, Nuclear Medicine and PET, Uppsala University, Uppsala, Sweden; [2]Hermes Medical Solutions, Stockholm, Sweden; [3]Division of Clinical Geriatrics, Department of Neurobiology, Care Sciences and Society, Karolinska Institutet, Huddinge, Sweden; [4]Department of Nuclear Medicine, Karolinska University Hospital, Huddinge, Sweden; [5]Theme Aging, Karolinska University Hospital, Huddinge, Sweden

[*]First author and corresponding author:

Johan Lilja, PhD

Address: Akademiska sjukhuset, 751 85 Uppsala, Sweden

Phone: +46733755601, Fax: +46184712000,

E-Mail: johan.lilja@radiol.uu.se

Running title: Normalization of ^{18}F-flutemetamol PET

Word count: 4663

Financial support: ^{18}F-Flutemetamol data collected in the validation cohort was largely sponsored by Vinnova - the Swedish Governmental Agency for Innovation Systems, grant number 2013-05175.

ABSTRACT

Though currently approved for visual assessment only, there is evidence to suggest that quantification of amyloid-β (Aβ) PET images may reduce inter-reader variability and aid in the monitoring of treatment effects in clinical trials. Quantification typically involves a regional atlas in standard space, requiring PET images to be spatially normalized. Different uptake patterns in Aβ-positive and Aβ-negative subjects, however, makes spatial normalization challenging. In this study we propose a method to spatially normalize ^{18}F-flutemetamol images, using a synthetic template based on principal component images to overcome these challenges. **Methods:** ^{18}F-Flutemetamol PET and corresponding MR images from a phase II trial (n=70), including subjects ranging from Aβ-negative to Aβ-positive, were spatially normalized to standard space using an MR driven registration method (SPM12). ^{18}F-Flutemetamol images were then intensity normalized using the pons as reference region. Principal component images were calculated from the intensity normalized images. A linear combination of the first two principal component images was then used to model a synthetic template, spanning the whole range from Aβ-negative to Aβ-positive. The synthetic template was then incorporated in our registration method, where the optimal template was calculated as part of the registration process, providing a PET only driven registration method. Evaluation of the method was done in two steps. First, co-registered gray matter masks generated using SPM12 were spatially normalized using the PET and MR driven methods, respectively. The spatially normalized gray matter masks were then visually inspected and quantified. Secondly, to quantitatively compare the two registration methods, additional data from an ongoing study were spatially normalized using both methods with correlation analysis on the resulting cortical SUVR values. **Results:** All scans were successfully spatially normalized using the proposed method, with no manual adjustments performed. Both

visual and quantitative comparison between the PET and MR driven methods showed high agreement in cortical regions. ^{18}F-Flutemetamol quantification showed strong agreement between the SUVR values for the PET and MR driven methods (R^2=0.996; pons reference region).
Conclusion: The principal component template registration method allows for robust and accurate registration of ^{18}F-flutemetamol images to a standardized template space, without the need for an MR image.

Keywords: Alzheimer's disease, amyloid-β, PET, ^{18}F-flutemetamol, adaptive template

INTRODUCTION

Following the first successful study using the carbon-11 labelled amyloid-β (Aβ) selective ligand Pittsburgh compound-B (^{11}C-PIB) (*1*), Aβ imaging with positron emission tomography (PET) has exerted a rapid and extensive influence on Alzheimer's disease (AD) research. As a result of the short half-life of the carbon-11 radioisotope, however, an onsite cyclotron and specialized radiochemistry infrastructure are required, limiting the utility of ^{11}C-PIB as a clinical diagnostic tool. As such, a number of Aβ specific PET tracers radiolabeled with the longer-lived fluorine-18 radioisotope have been developed for clinical applications. To date, three such compounds have been approved by the Food and Drug Administration and European Medicines Agency, including ^{18}F-florbetapir (*2,3*), ^{18}F-florbetaben (*4,5*), and ^{18}F-flutemetamol (*6,7*).

Though currently validated for visual assessment only, in which scans are classified as negative (normal) or positive (abnormal) by a trained reader, there is evidence to suggest that the incorporation of quantitative approaches for use with currently approved Aβ imaging PET tracers may reduce inter-reader variability (*8*), and aid with respect to the monitoring of treatment effects from anti-Aβ drugs (*9*). Quantification typically involves computation of a standardized uptake value ratio (SUVR), in which late duration tracer uptake within target regions is normalized to that within a reference tissue, such as the cerebellum or pons (*1,3,4,7*). As a requisite for SUVR computation, a PET image must first be parcellated into anatomically meaningful regions; the gold standard for this type of approach requires access to a subject's T1-weighted magnetic resonance (MR) image, and manual delineation of volumes on interest (VOIs) in native space. This method, however, is time consuming and may be subject to inter-reader variability; further, structural imaging with can prove challenging to obtain in clinical settings. As such, PET-only approaches have been developed, where, following normalization to a reference space, division

of the Aβ image into VOIs and subsequent calculation of SUVR is achieved using a computer generated, predefined regional atlas.

One of the challenges inherent to current fluorine-18 Aβ PET tracers lies in their capacity for high uptake in both gray and white matter. Though increased cortical uptake occurs in proportion to fibrillary Aβ levels, nonspecific white matter uptake is characteristically seen, regardless of fibrillary Aβ load (Fig. 1). The different patterns of uptake across Aβ-positive (Aβ+) and negative (Aβ-) images can, therefore, result in a systematic bias when using a standard, single template, PET driven registration method. Though utilization of a subject's MR image stands as a possible solution to this challenge, MR imaging is not always available as part of routine clinical workup, highlighting the relevance of a PET based method able to resolve the bias imposed by variability in Aβ ligand uptake.

To overcome the problems outlined above, we developed a fully automated PET only registration method utilizing a synthetic template based on principal component images. In this approach, the linear combination of the first and second components from a principal decomposition analysis of ^{18}F-flutemetamol images were used to model a synthetic template, spanning the whole range from Aβ- to Aβ+. The synthetic template was then used to drive registration to standard space. Here, we describe the creation of the principal component template model, its integration into an image registration algorithm, and the validation of our method against an MR driven approach for spatial normalization (SPM12).

MATERIAL AND METHODS

Subject and Imaging

The study population consisted of 117 subjects, divided across two cohorts: a template creation cohort and a registration validation cohort (Table 1). The template creation cohort consisted of 70 subjects (25 cognitively normal healthy volunteers, 19 amnestic mild cognitive impairment (aMCI), 26 AD) from a ^{18}F-flutemetamol phase II study (*6*), approved by Ethical Committees of the participating sites. The registration validation cohort consisted of 47 patients (14 MCI, 27 AD, 5 non-AD, and one case of dementia not otherwise specified) from an ongoing study at the Karolinska University Hospital, Huddinge, Sweden, investigating the clinical utility of ^{18}F-flutemetamol PET in patients with an unclear diagnosis. The Regional Human Ethics Committee of Stockholm, Sweden, and the Isotope Committee of Karolinska University Hospital Huddinge approved this study. For both studies, all patients gave their written informed consent.

Data from the template creation cohort was used to create the principal component templates and to evaluate the image registration method while data from the registration validation cohort was used to validate the spatial normalization. For the template creation cohort, the ^{18}F-flutemetamol PET imaging protocol consisted of 6x5 minutes frames, 85 minutes post injection of approximately 180 MBq, with scanning performed at three different centers, using three different scanners (Biograph PET/CT and ECAT EXACT HR+ (Siemens) and GE Advance); structural T1-weighted MR imaging data was acquired for all subjects. For the registration validation cohort, the ^{18}F-flutemetamol protocol consisted of a 20 minute (list-mode) scan, 90 minutes post injection of approximately 185 MBq (Siemens Biograph mCT PET/CT). Structural T1-weighted MR imaging data was acquired at several radiology departments in Stockholm and neighboring counties, with different platforms and protocols.

Reference Space and Anatomic Regions

The Montreal Neurology Institute (MNI) space was used as a references space, together with the 1-mm isotropic T1-weighted MR template from the International Consortium of Brain Mapping (ICBM) (*10*). The following VOIs were adapted from the Centiloid project (*11*), a recently proposed method aiming to facilitate comparison and combination of Aβ PET data through the use of a linear scaling procedure: Cerebellar Gray (CG), Whole Cerebellum (WC), Whole Cerebellum plus Brainstem (WC+B), Pons and Global Cortical Target (CTX). Included in the CTX meta-VOI were brain regions known to typically display a high load of amyloid, including the frontal, temporal and parietal cortices, as well as the precuneus, anterior striatum, and insular cortex (*11*). In addition, we added a fifth VOI by modifying the Centiloid Pons VOI through the selection of only those voxels containing high ^{18}F-flutemetamol uptake (Fig. 2). This threshold version of the Centiloid Pons is referred to as ThPons.

Principal Components Template and Spatial Normalization

Principal component analysis (PCA) is a statistical technique to investigate the variance-covariance structure of a set of variables. In general, PCA serves two purposes: data reduction and interpretation. Working with high dimensional data, PCA may be a good way of reducing dimensionality of data and by that finding relationships that would otherwise be hard to find. Given n images with $p = rows \times cols \times slices$ voxels a matrix $\mathbf{X}^{p\times n}$ can be formed. The (unbiased) sample variance-covariance matrix, $\mathbf{C}^{n\times n}$, of $\mathbf{X}$ can then be calculated as

$$\mathbf{C} = \frac{\mathbf{D}'\mathbf{D}}{n-1}$$

where $\mathbf{D}^{p\times n} = (\mathbf{X}^{p\times n} - \boldsymbol{\mu}^{p\times 1}\mathbf{1}^{1\times n})$ where $\mathbf{1}^{1\times n}$ is a row vector of ones and $\boldsymbol{\mu}$ is simply the mean image where voxel i (i=1,…,p) is calculated as

$$\mu_i = \frac{1}{n}\sum_{i=1}^{n} x_i$$

The voxel based principal components can then be calculated using singular value decomposition (SVD)

$$\mathbf{C} = \mathbf{V}\mathbf{\Lambda}\mathbf{V}'$$

where $\mathbf{V}^{n\times n}$ is the eigenvector matrix who's i^{th} (i=1,…,n) column is the eigenvector, $\mathbf{q_i}$, $\mathbf{\Lambda}^{n\times n}$ is the diagonal matrix whose diagonal elements, λ_i, are the corresponding eigenvalues and $\mathbf{V}'$ is the transpose of $\mathbf{V}$. A principal component image, I_{PCi}, is then calculated by multiplying $\mathbf{D}$ with one of its eigenvectors, $\mathbf{q_i}$:

$$I_{PCi} = \mathbf{D} \times \mathbf{q_i}$$

First, all MR and corresponding ^{18}F-lutemetamol images were co-registered. We then spatially normalized all images to the MNI space using the MR driven registration provided by SPM12. Images were then intensity normalized using the Pons region. To make sure the images in the template creation cohort spanned the whole range from Aβ- to Aβ+ we calculated the cortical SUVR values using the CTX as target region and Pons as reference region (Fig. 3). SUVR findings for the registration validation cohort are shown in Supplemental Fig. 1.

Principal component images for all 70 spatially and intensity normalized ^{18}F-flutemetamol images in the template creation cohort were calculated. Principal component images were then sorted based on their eigenvalues to determine the order of significance for each component. We decided to use the first two principal components, explaining 94.6% of the variance, to generate a synthetic template. Any number of components could be used, but since the remaining 68, higher order, components only describe an accumulated variance of 5.4% of the total variance, they were considered not to contribute with much relevant information regarding image registration. Fig. 4 shows trans-axial, coronal and sagittal views of the first

principal component image (I_{PC1}) (top row) and the second principal component image (I_{PC2}) (bottom row) using the recommended rainbow color scale (*12*).

A synthetic template image, $I_{synthetic}$, could now be modelled by a linear combination of I_{PC1} and I_{PC2} where a weight, w, ranging from -1.0 to 1.0 is multiplied with I_{PC2} according to:

$$I_{synthetic} = I_{PCA1} + wI_{PCA2}$$

A value of weight w of -1.0 will correspond to an Aβ- subject whereas a value of 1.0 will correspond to an Aβ+ subject. Fig. 5 shows the range of the synthetic template images across the range (-1.0 to 1.0) of possible w values.

A registration method was developed allowing the weight w to be incorporated in the optimization method together with the parameters for spatial transformation as described by Thurfjell at al. (*13*). This allows the registration method to iteratively find the best set of spatial transformation parameters for a patient's ^{18}F-flutemetamol scan to fit the optimal template for this particular scan. As an initial step, a multi resolution global 12 parameter affine registration is used. When the global registration has converged, a brain mask without ventricles is used to refine the registration of the cortical areas of the brain by continuing to improve the affine transform as well as by adding a higher order deformation in the form of a second order polynomial transformation (*14*). Once converged, refinement of the registration of the brainstem and cerebellum is performed. For the first two steps, normalized mutual information was used as similarity metric, whereas for the last step, normalized cross correlation was used. Powell's algorithm (*15*) was used for optimization throughout the whole registration.

Refined Registration of Pons and Cerebellum

The quality of the registration of the reference region is important for quantification of Aβ images. Because of the low anatomical information in Aβ PET images a registration method with a high number of degrees of freedoms may not be feasible. The constraints of the second order polynomial deformation field may on the other hand not be sufficient to get a good local registration of the reference regions. Because of this we added a final registration step to the registration algorithm where we allow for a 6 parameters rigid registration of the pons and cerebellum. A volumetric binary mask covering the whole cerebellum and brain stem was created. The mask was then smoothed using a 3-dimensional Gaussian filter (Fig. 6A). When registering the reference region, not all voxels within the mask were used but rather it was subsampled by thresholding $I_{synthetic}$ using only the characteristic high uptake voxels to drive the registration. The threshold was determined by calculating an intensity histogram for all voxels of $I_{synthetic}$ within the cerebellum and brain stem mask, and then calculating the voxel value at 85% of the intensity histogram (Fig. 6B). The calculated transform is then applied using to the whole cerebellum and brain stem mask. To avoid discontinuities in the final transformed image, the smoothed mask is used as a weight for the calculated transform where values completely outside the mask are not affected and values within the mask will be affected in the order of the value in the smoothed mask, ranging from 0.0 to 1.0 where a value of 1.0 means that the calculated transform is fully applied.

Experiments

Co-registered ^{18}F-flutemetamol images were spatially normalized to the MNI T1 Template in two ways: first, using transforms derived by MR driven registration as provided by SPM12

(http://www.fil.ion.ucl.ac.uk/spm) and second, using the principal component template registration method.

Quality of Spatial Normalization

Using spatially normalized MR images from the template creation cohort, gray and white matter probabilistic tissue masks were created for both registration methods. The amount of gray matter and white matter in CG and CTX VOIs was calculated based on the probabilistic tissue maps. Paired t-tests using a commercial software package (Matlab, R2016a, The MathWorks Inc) was performed to evaluate differences in the amount of gray matter and white matter in CG and CTX VOIs between the two registration methods. Mean gray matter images for Aβ- and Aβ+ images were then created for each registration method (Fig. 7), with images then visually inspected for systematic differences in registration quality tied to Aβ status (negative, positive).

Quantitative Comparison with MR Driven Registration

For both the template creation and validation cohorts, cortical SUVR values were calculated using all reference regions, using both registration methods. The correlation between MR driven and principal component template registration methods was then calculated separately for each cohort.

RESULTS

Quality of Spatial Normalization

All scans were successfully spatially normalized, with no manual adjustments performed. The amount of gray matter in the CG VOI was higher for the principal component template approach ($p<0.001$), while the amount of white matter was lower ($p<0.001$) (Supplemental Fig. 2A and B).

Similar results were found when using the CTX VOI ($p<0.001$) (Supplemental Fig. 2C and D). For both regions, the principal component template registration method yielded lower variance in the results in the amount of gray and white matter, respectively.

Visual inspection of the mean gray matter images created from the SPM12 registered MR images did not show any apparent systematic differences between Aβ- and Aβ+; nor did the mean gray matter images created using the principal component template registration method. Further, we could not see any apparent differences between the two registration methods based on the visual inspection of the gray matter mean images for Aβ- and Aβ+ images, respectively.

Quantitative Comparison with MR Driven Registration

Comparison of quantification results using ^{18}F-flutemetamol driven principal component template registration and MR driven SPM12 registration showed good agreement (Table 2).
For the registration validation cohort, the coefficient of determination, R^2, between SUVRs for the CTX region computed with both methods ranged from 0.984 with CG as reference region, to 0.996 using ThPons as reference region (Supplemental Fig. 3).

By visual inspection, it was noted that two subjects, A and B, in the registration validation cohort, had a better fit to Pons using the principal component registration, compared with the SPM12 registration (Supplemental Fig. 4). Removing these two subjects from the analysis gave an R^2 value of 0.993 using the Pons as reference region.

DISCUSSION

Quantification of tracer uptake has the potential of aiding clinicians in the interpretation of Aβ PET images, as a complement to visual assessment. This approach can increase clinical

confidence, particularly in cases where the images are difficult to interpret. For this, regions of interest as well as reference regions needs to be defined to provide the image interpreter with a quantitative measure unaffected by parameters such as the administered dose or patient body composition. Commonly, this is done through spatial normalization of the images to a template space, in which a pre-defined atlas can be applied to estimate SUVR. However, bi-modal appearance of Aβ imaging (*16*) presents a well-known obstacle to the use of single-modality spatial normalization of PET images to a template space, since the use of a common PET template image for both positive and negative images commonly leads to sub-optimal registration due to the completely different image characteristics.

We have here demonstrated the implementation and creation of a synthetic Aβ template, using principal component decomposition of a set of Aβ scans, ranging from Aβ- to Aβ+, registered to the MNI space. Even though it would be possible to use a larger number of components, the synthetic template was created using a linear combination of the first two principal components, excluding the higher order components that contributed minimally to image appearance. The second order component was identified as being responsible for the signal related to specific binding, thus representing the difference between positive and negative images. As seen in Fig. 4 this component accurately identifies cortical regions associated with Aβ binding, excluding motor, visual and cerebellar cortices. In our template creation procedure, the weight of this component is determined iteratively during the image registration procedure, resulting in a template with an optimal likeness to the positive-negative range from the patient data being normalized. This also has the advantage that the registration to the template of the patient image is performed using a template with similar image characteristics as the patient image, improving registration quality.

The proposed method focuses on the accuracy of the registration of cortical and reference regions. Using a global deformation field, as provided by the second order polynomial transform having relatively few degrees of freedom, it is possible to compensate for global differences in anatomy. However, we noticed that the size of the ventricles varied across subjects, and, as a precaution, to avoid any potential bias in the registration, the ventricles were not included in the final step of the global registration, limiting the performance of the registration around the ventricles.

Although compensating for global differences in anatomy, the global deformation field may not be able to compensate for differences in the reference regions. Because of this, we introduced a final registration step allowing for refinement of the registration of the reference regions. An interesting finding is the quality of the registration of the reference regions in subject A and B, where we believe the proposed method shows a more accurate registration than the reference method. This may be due to the choice of reference method, where the MR-driven registration provided by SPM12 is only allowing for a global deformation field using a linear combination of low frequency basis functions.

Diagnosing pathological Aβ binding using PET at the individual patient level was recently shown to have a significant impact on diagnostic confidence and drug treatment (*17-19*). The PET-based diagnosis is currently a dichotomous process performed using visual criteria. Cases with borderline changes are often difficult to classify visually in a clinical routine setting, especially for readers without extensive experience. Further, disease modifying drugs targeting Aβ plaques may have only modest effects on brain levels, resulting in changes to the Aβ PET signal that are not visually apparent. Automated quantification using the proposed method might increase reader certainty and further the clinical adoption of Aβ imaging, including within the context of clinical trials. Moreover, since the method proposed here appears to be at least as

accurate as the dual-scan concept used by the gold standard SPM12, the new method might simplify such studies by removing the need for a separate MRI scan. Further, due to the choice of data for the generation of the template as well as for validation, the method may be considered insensitive to reconstruction method and scanner type.

Other methods using adaptive templates (*13*) and principal component derived templates (*20*) have been proposed for ^{11}C-PIB and ^{18}F-flutemetamol, respectively. In the study by Fripp et al. (*20*), though they, similar to our method, used a principal component approach to generate an adaptive template, spline based transformations were used for the normalization step; as a result, their approach carries a heavy computational cost (> 6 hours). By comparison, an average processing time of 20 seconds is required to process a subject using our method. Further, our work extends that of Fripp et al., showing that a principal component driven template approach can be successfully implemented with ^{18}F-flutemetamol and, possibly, additional approved fluorine-18 Aβ tracers. In the study by Lundqvist and colleagues (*13*), linear regression was used to generated intercept (fixed) and slope images; the latter, in combination with a weighting factor, was then used to generate a template. Though their regression derived slope image provides a measure similar to our second principal component image, visual comparison of resulting templates suggests greater accuracy with our proposed method. Moreover, in contrast to their method, for which a patent is pending (21), our approach is unpatented, potentially facilitating collaborative projects aiming to validate our template using additional Aβ tracers.

CONCLUSION

The proposed method allows for robust and accurate registration of ^{18}F-flutemetamol images to template space, without additional imaging procedures. This might simplify the clinical use of quantification in Aβ PET imaging. A promising strategy, the use of adaptive templates may be expanded to other tracers with potential clinical applications, such as those for tau or dopamine synthesis and transport.

DISCLOSURE

The ^{18}F-flutemetamol phase II study was designed and sponsored by GE Healthcare. The majority of the ^{18}F-lutemetamol data in the registration validation cohort was sponsored by Vinnova - the Swedish Governmental Agency for Innovation Systems, grant number 2013-05175. Johan Lilja is a former employee of GE Healthcare and currently holds a position at Hermes Medical Solutions.

REFERENCES

1. Klunk WE, Engler H, Nordberg A, et al. Imaging brain amyloid in Alzheimer's disease with Pittsburgh Compound-B. *Ann Neurol.* 2004;55:306-319.

2. Clark CM, Schneider JA, Bedell BJ, et al. Use of florbetapir-PET for imaging beta-amyloid pathology. *JAMA.* 2011;305:275-283.

3. Wong DF, Rosenberg PB, Zhou Y, et al. In vivo imaging of amyloid deposition in Alzheimer disease using the radioligand 18F-AV-45 (florbetapir [corrected] F 18). *J Nucl Med.* 2010;51:913-920.

4. Villemagne VL, Ong K, Mulligan RS, et al. Amyloid imaging with (18)F-florbetaben in Alzheimer disease and other dementias. *J Nucl Med.* 2011;52:1210-1217.

5. Barthel H, Gertz HJ, Dresel S, et al. Cerebral amyloid-beta PET with florbetaben (18F) in patients with Alzheimer's disease and healthy controls: a multicentre phase 2 diagnostic study. *Lancet Neurol.* 2011;10:424-435.

6. Vandenberghe R, Van Laere K, Ivanoiu A, et al. 18F-flutemetamol amyloid imaging in Alzheimer disease and mild cognitive impairment: a phase 2 trial. *Ann Neurol.* 2010;68:319-329.

7. Nelissen N, Van Laere K, Thurfjell L, et al. Phase 1 study of the Pittsburgh compound B derivative 18F-flutemetamol in healthy volunteers and patients with probable Alzheimer disease. *J Nucl Med.* 2009;50:1251-1259.

8. Nayate AP, Dubroff JG, Schmitt JE, et al. Use of Standardized Uptake Value Ratios Decreases Interreader Variability of [18F] Florbetapir PET Brain Scan Interpretation. *AJNR Am J Neuroradiol.* 2015;36:1237-1244.

9. Schmidt ME, Chiao P, Klein G, et al. The influence of biological and technical factors on quantitative analysis of amyloid PET: points to consider and recommendations for controlling variability in longitudinal data. *Alzheimers Dement.* 2015;11:1050-1068.

10. ICBM-152 template. http://packages.bic.mni.mcgill.ca/tgz/mni-models_icbm152-lin-1.0.tar.gz. Accessed on Dec 15, 2017.

11. Klunk WE, Koeppe RA, Price JC, et al. The Centiloid Project: standardizing quantitative amyloid plaque estimation by PET. *Alzheimers Dement.* 2015;11:1-15 e11-14.

12. Summary of Product Characteristics, Vizamyl. http://www.ema.europa.eu/docs/en_GB/document_library/EPAR_Product_Information/human/002557/WC500172950.pdf. Accessed on Dec 12, 2017.

13. Lundqvist R, Lilja J, Thomas BA, et al. Implementation and validation of an adaptive template registration method for 18F-flutemetamol imaging data. *J Nucl Med.* 2013;54:1472-1478.

14. Woods RP, Grafton ST, Watson JD, Sicotte NL, Mazziotta JC. Automated image registration: II. Intersubject validation of linear and nonlinear models. *J Comput Assist Tomogr.* 1998;22:153-165.

15. Powell MJD. An efficient method for finding the minimum of a function of several variables without calculating derivatives. *Comput. J* 1964;7:155-162.

16. Klunk WE. Amyloid imaging as a biomarker for cerebral beta-amyloidosis and risk prediction for Alzheimer dementia. *Neurobiol Aging.* 2011;32 Suppl 1:S20-36.

17. Boccardi M, Altomare D, Ferrari C, et al. Assessment of the Incremental Diagnostic Value of Florbetapir F 18 Imaging in Patients With Cognitive Impairment: The Incremental Diagnostic Value of Amyloid PET With [18F]-Florbetapir (INDIA-FBP) Study. *JAMA Neurol.* 2016;73:1417-1424.

18. Ceccaldi M, Jonveaux T, Verger A, et al. Added value of (18)F-florbetaben amyloid PET in the diagnostic workup of most complex patients with dementia in France: A naturalistic study. Alzheimers Dement. 2018;14:293-305.

19. de Wilde A, van Maurik IS, Kunneman M, et al. Alzheimer's biomarkers in daily practice (ABIDE) project: Rationale and design. *Alzheimers Dement (Amst).* 2017;6:143-151.

20. Fripp J, Bourgeat P, Raniga P, et al. MR-less high dimensional spatial normalization of 11C PiB PET images on a population of elderly, mild cognitive impaired and Alzheimer disease patients. *Med Image Comput Comput Assist Interv.* 2008;11:442-449.

21. Lundqvist R, Thurfjell NL, Lilja J, et al. Methods of spatial normalization of positron emission tomography images 2013.

TABLES

Cohort	Groups	N	Age	Gender, M/F	MMSE
Template creation	HV	25	58 [44, 72]	12/13	-
	aMCI	19	71 [69, 80]	10/9	27, 30
	AD	26	72 [64.3, 74]	12/14	15, 26
Registration validation	MCI	14	60 [56, 64]	5/9	24, 29
	AD	27	66.5 [63.3, 73]	9/18	23, 26
	Non-AD	5	63 [62, 66]	2/3	24, 27
	Dementia NOS	1	63	1/0	22

Table 1. Demographic and clinical information for the template creation and validation cohorts. For age, data is presented as median [Quartile 1, Quartile 3]; for MMSE, the range of values is presented. HV, healthy volunteers. The non-AD group comprised three cases of vascular dementia and two of frontotemporal dementia. Dementia NOS, dementia not otherwise specified.

Reference Region	Cohort	R^2
CG	Template creation	0.978
	Registration validation	0.984
WC	Template creation	0.991
	Registration validation	0.992
WC+B	Template creation	0.993
	Registration validation	0.993
Pons	Template creation	0.993
	Registration validation	0.986 (0.993)
ThPons	Template creation	0.995
	Registration validation	0.996

Table 2. Correlation between SUVRs for CTX region computed with principal component template registration and SPM12. Number within parenthesis for the Pons region shows the results following removal of two subjects where visual assessment showed that principal component based registration was superior to SPM12 registration, based on fit to Centiloid Pons.

FIGURES

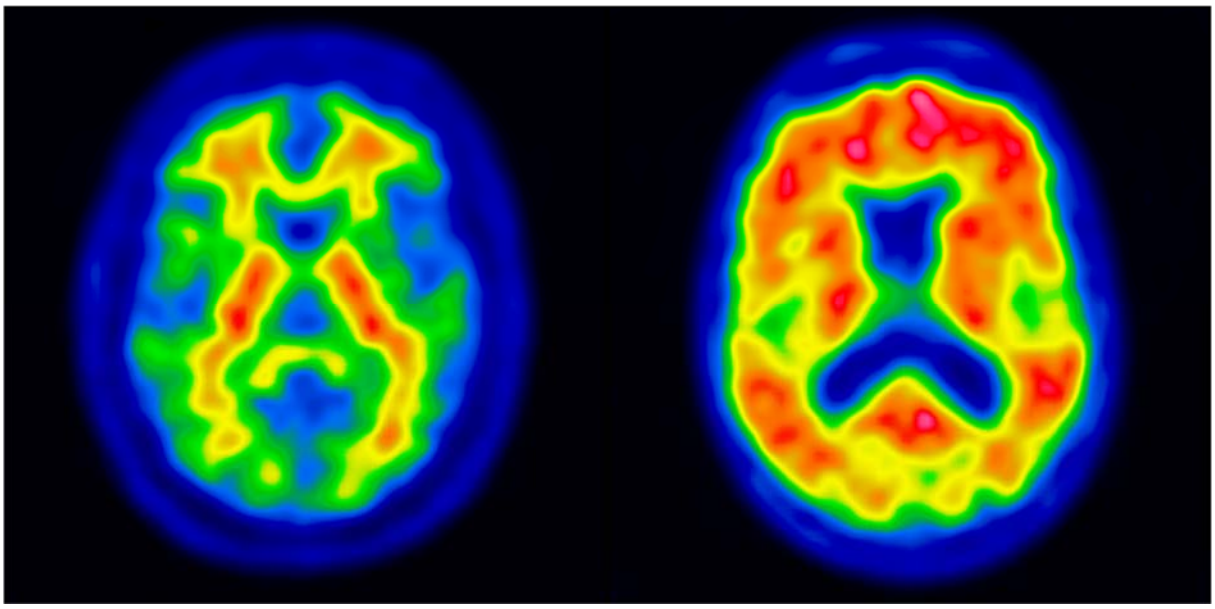

Fig. 1. Typical patterns of Aβ negative (Left) and positive (right) subjects.

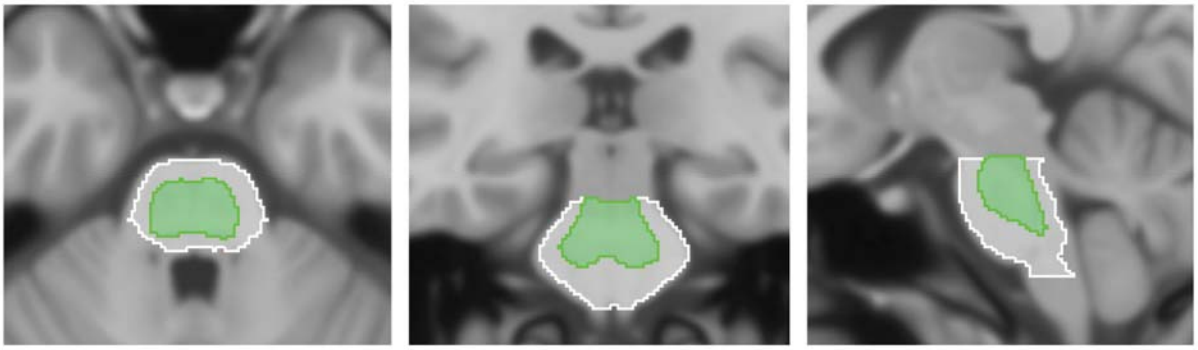

Fig. 2. Centiloid Pons (white) and a modified version of Centiloid Pons, ThPons (green), based on the voxels having the highest ^{18}F-flutemetamol uptake.

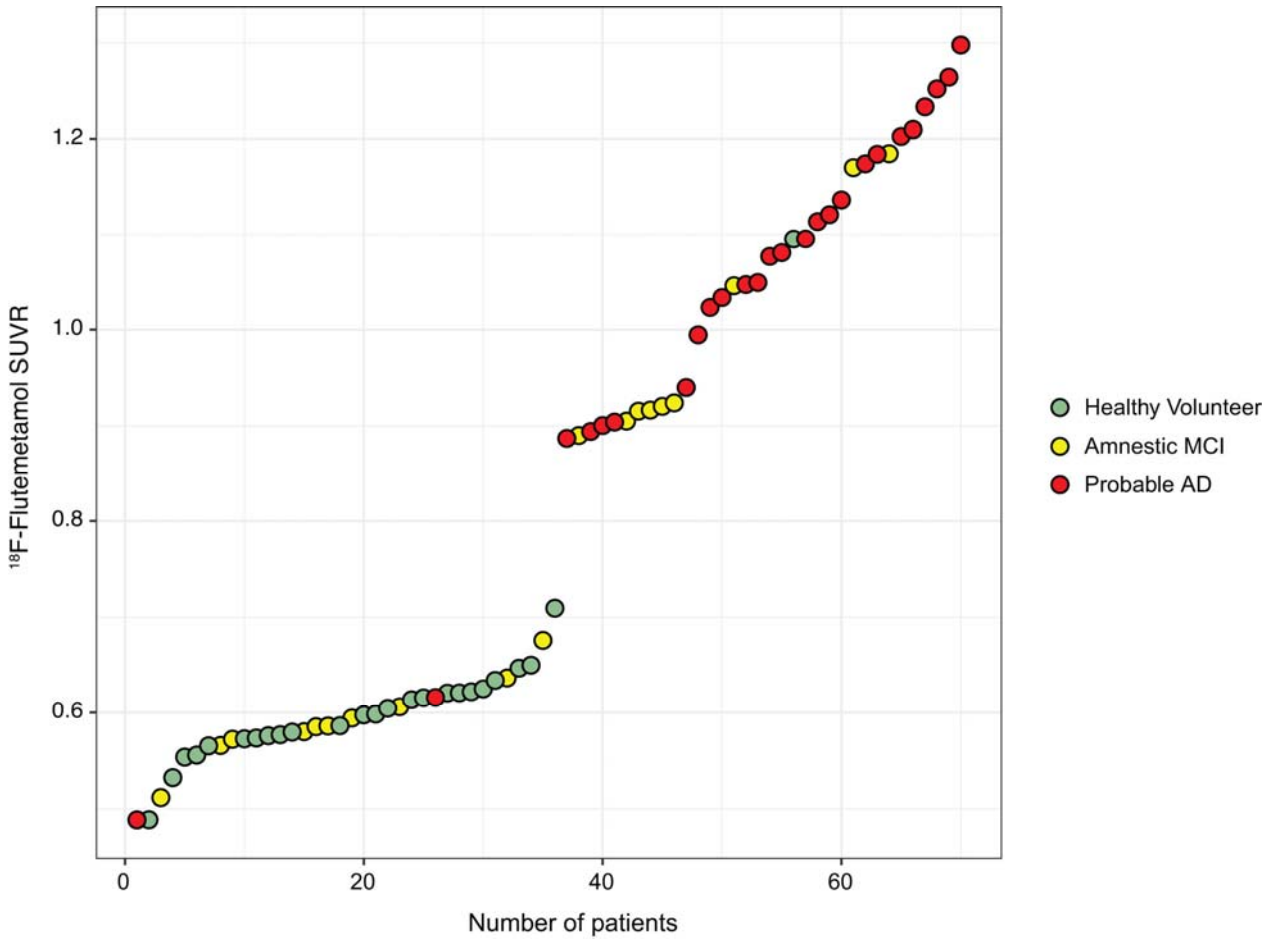

Fig. 3. ^{18}F-Flutemetamol CTX SUVR (using Pons as reference region) on the y-axis (template creation cohort) against patients, ranked according to SUVR, on the x-axis.

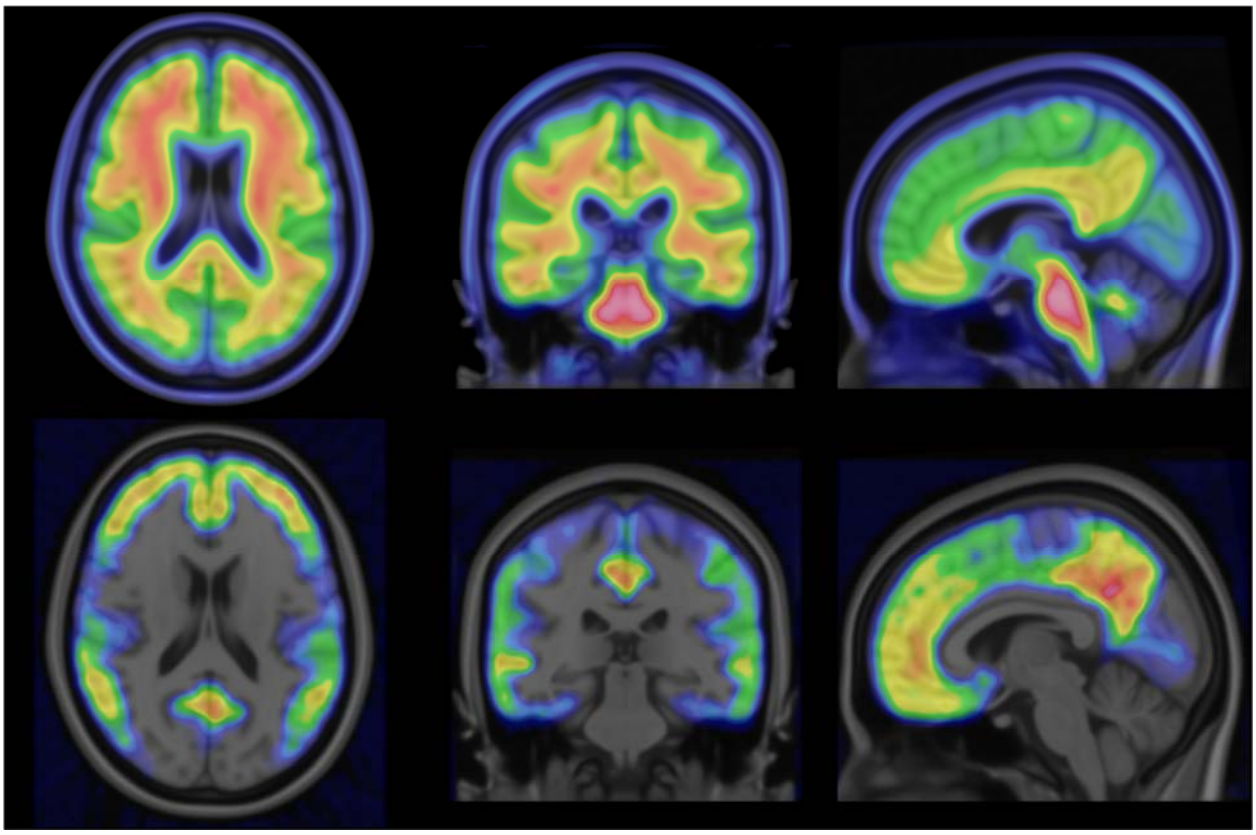

Fig. 4. From left to right: Axial, sagittal and coronal views of principal component image 1 (top row) and principal component image 2 (bottom row).

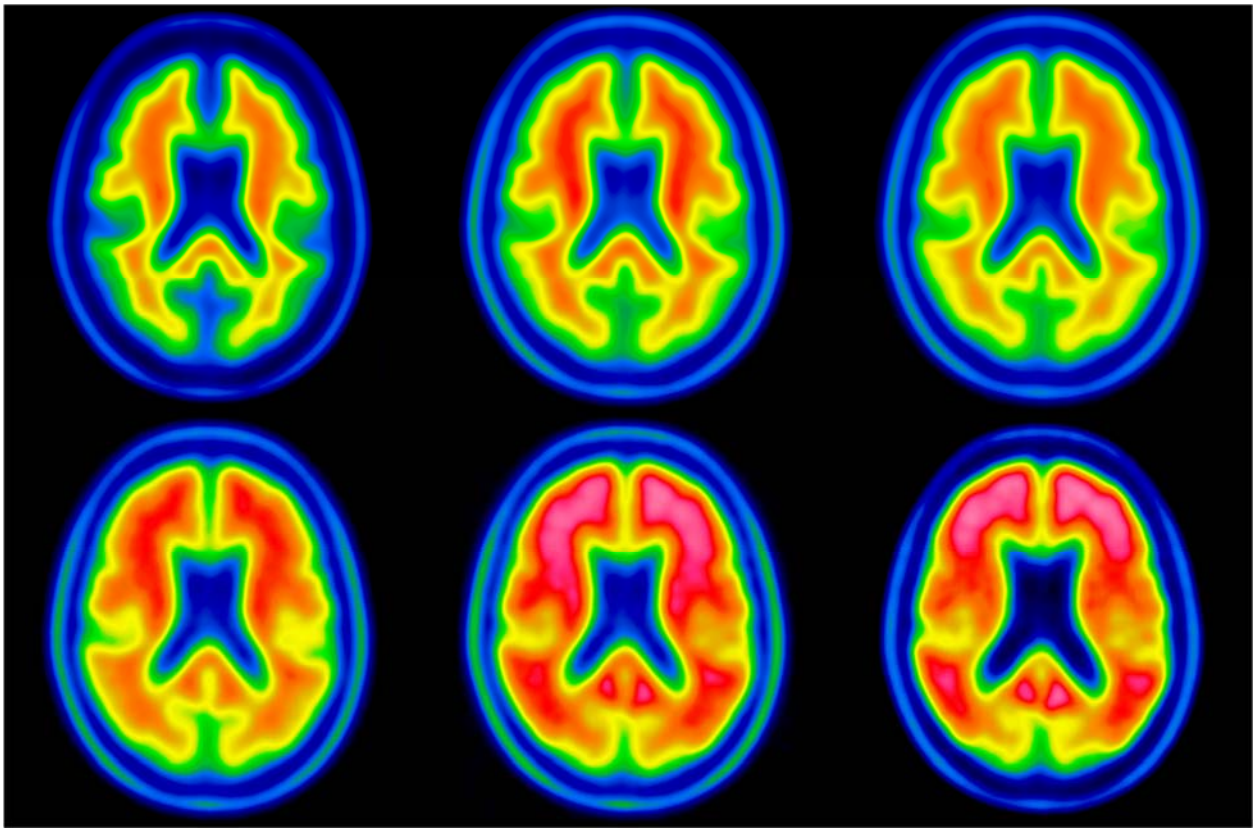

Fig. 5. Synthetic template images showing characteristic ^{18}F-flutemetamol uptake pattern going from most negative (upper left) to most positive case (lower right). The value of the weight, *w,* ranges from -1.0 (upper left) to 1.0 (lower right) and is increased by 0.4 going from left to right, top to bottom.

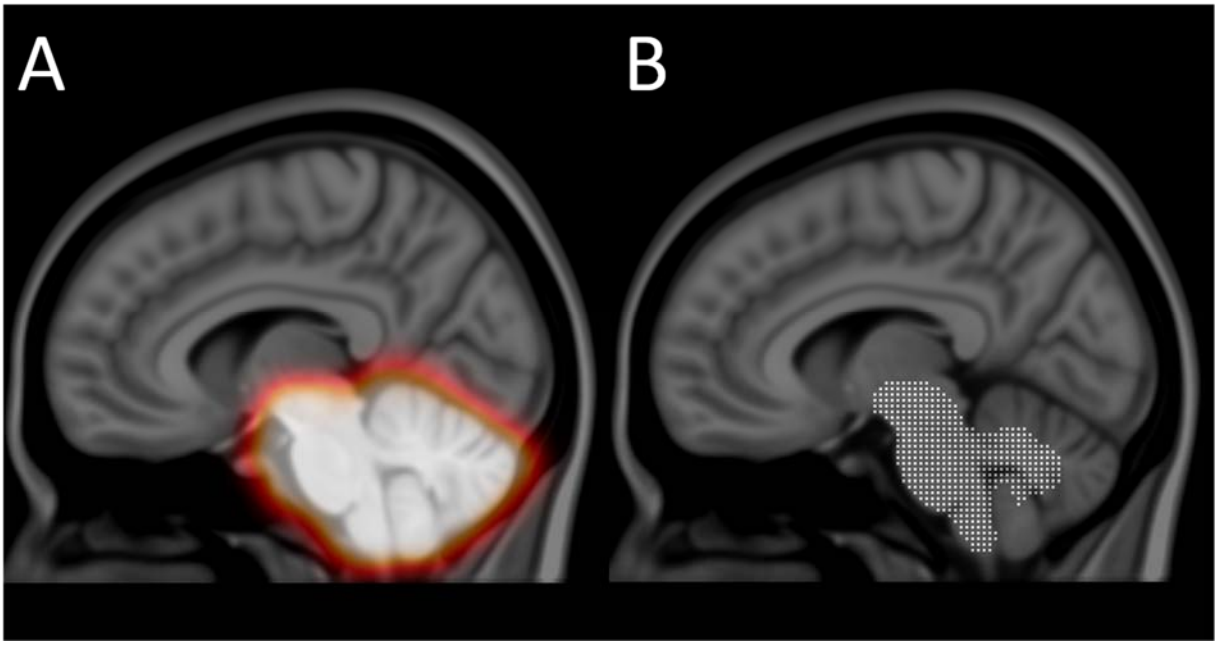

Fig. 6. Cerebellum and brain stem mask (A) and subsampling of high ^{18}F-flutemetamol uptake of cerebellum and brain stem mask (B).

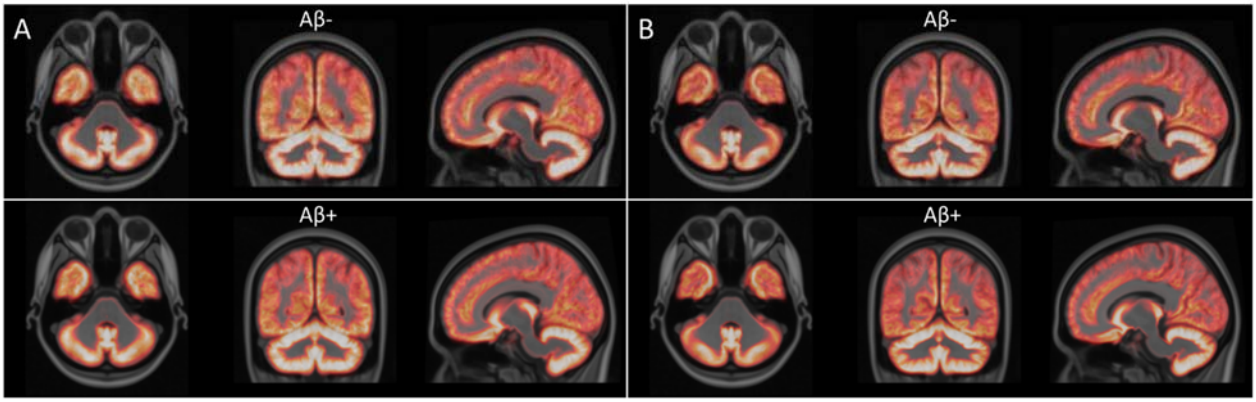

Fig. 7. Average gray matter probabilistic maps (template creation cohort) for Aβ negative (Aβ-) and positive (Aβ+) subjects using Principal Component Template Registration (A) and SPM12 registration (B) methods.

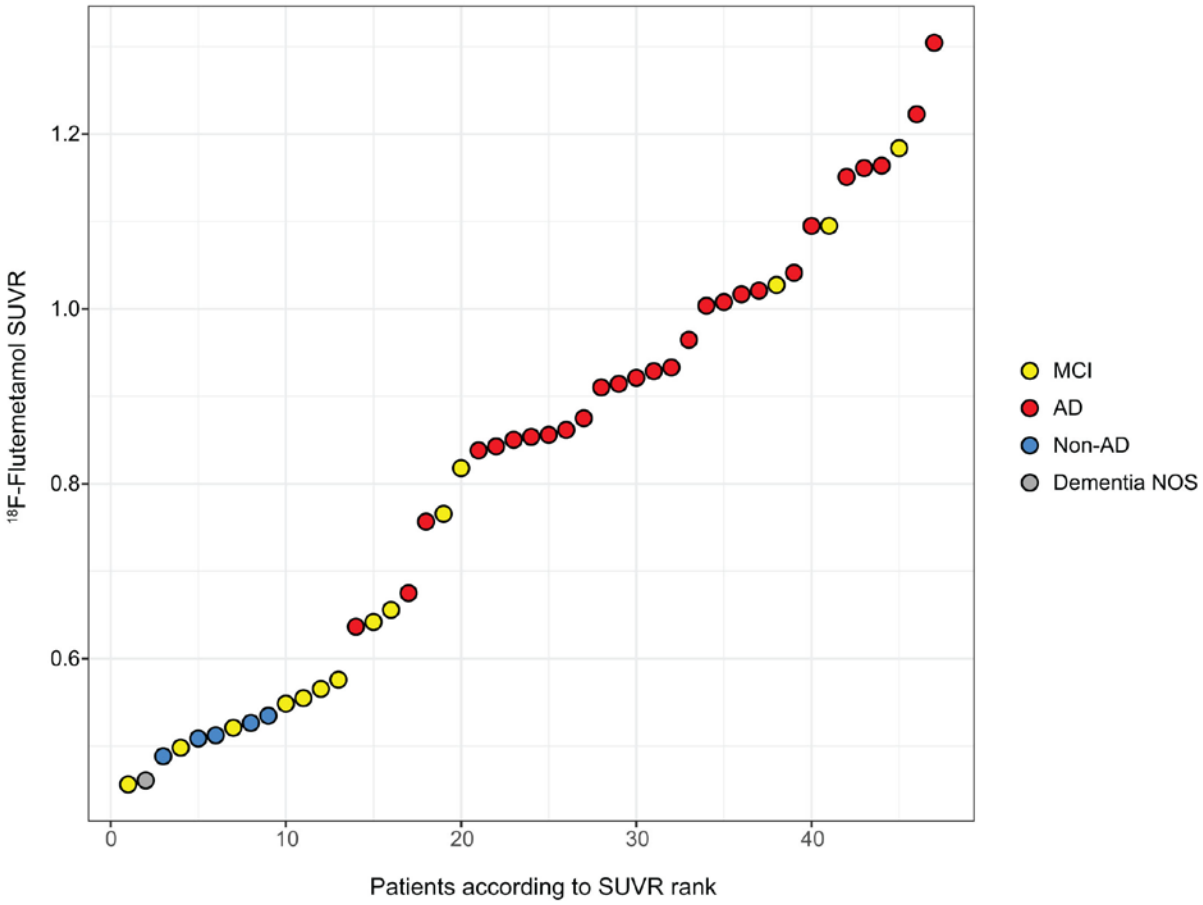

Supplemental Fig. 1. ^{18}F-Flutemetamol CTX SUVR (using Pons as reference region) on the y-axis (registration validation cohort) against patients, ranked according to SUVR, on the x-axis.

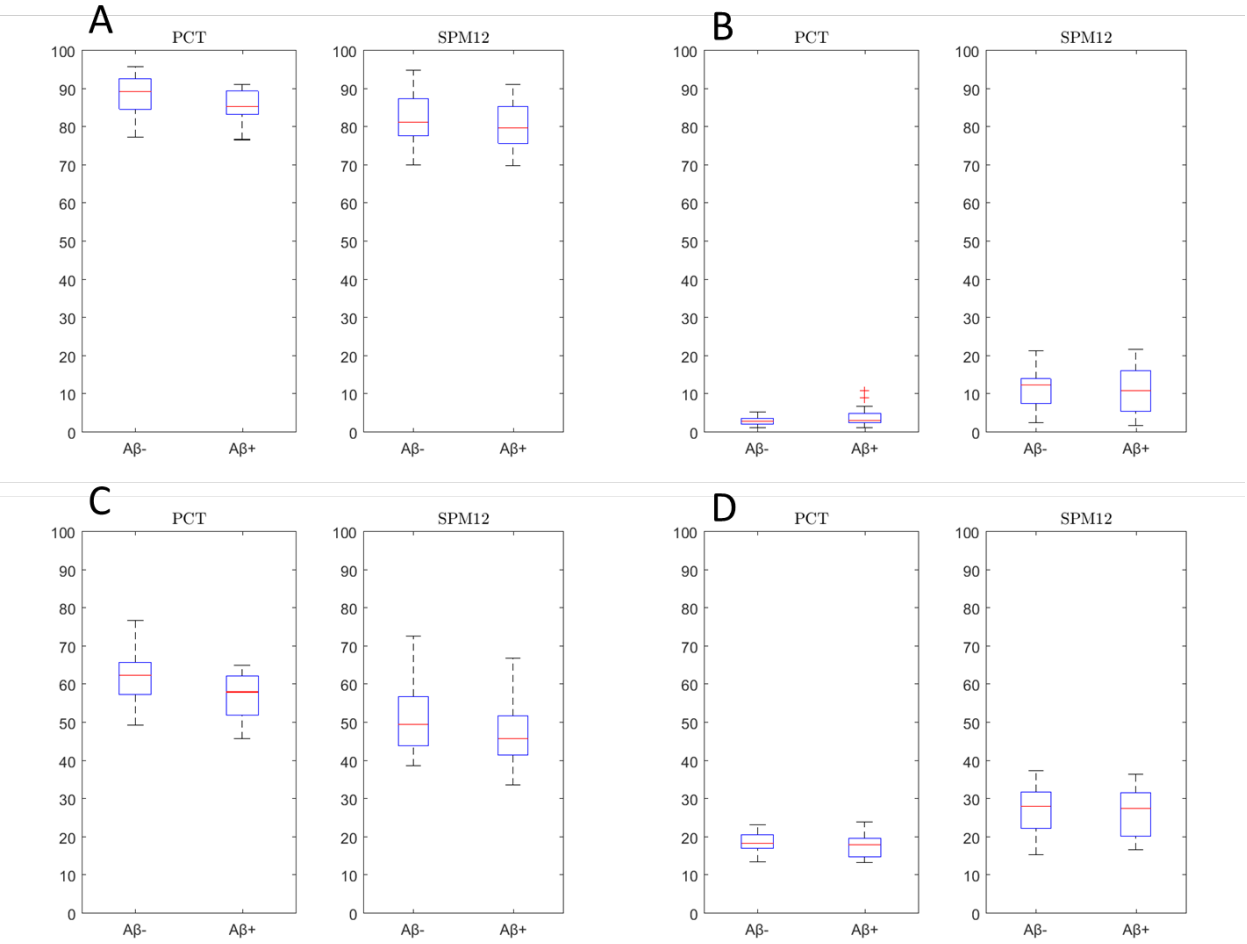

Supplemental Fig. 2. Original Cohort: Amount of gray matter (A) and white matter (B) in CG using Principal Component Template (PCT) and SPM12 registration. Amount of gray matter (C) and white matter (D) in CTX using Principal Component Template (PCT) and SPM12 registration.

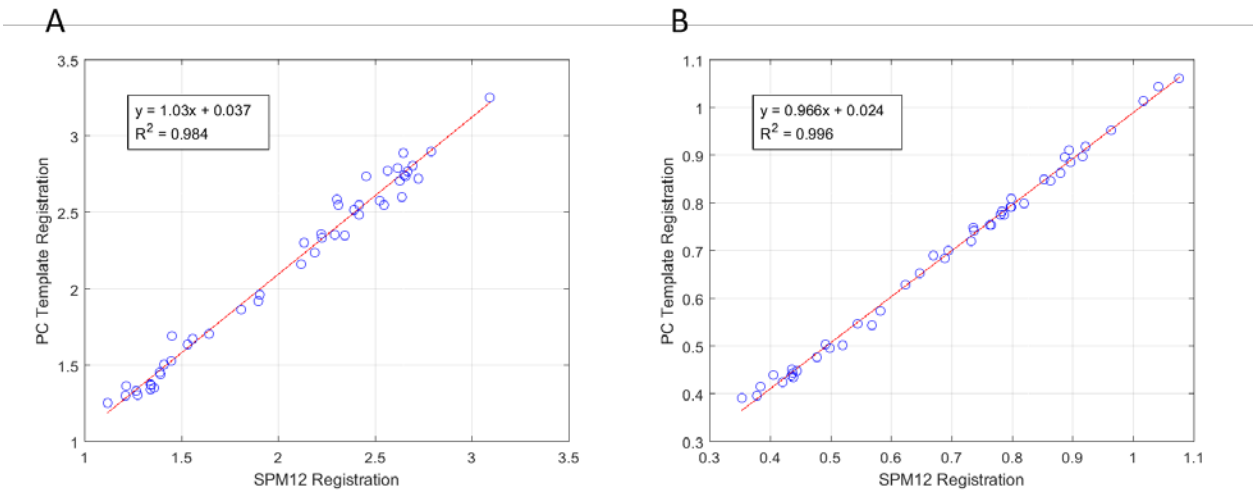

Supplemental Fig. 3. Validation Cohort: Correlation between SUVRs for CTX region computed with principal component template registration and SPM12 registration using CG as reference region (A) and ThPons as reference region (B).

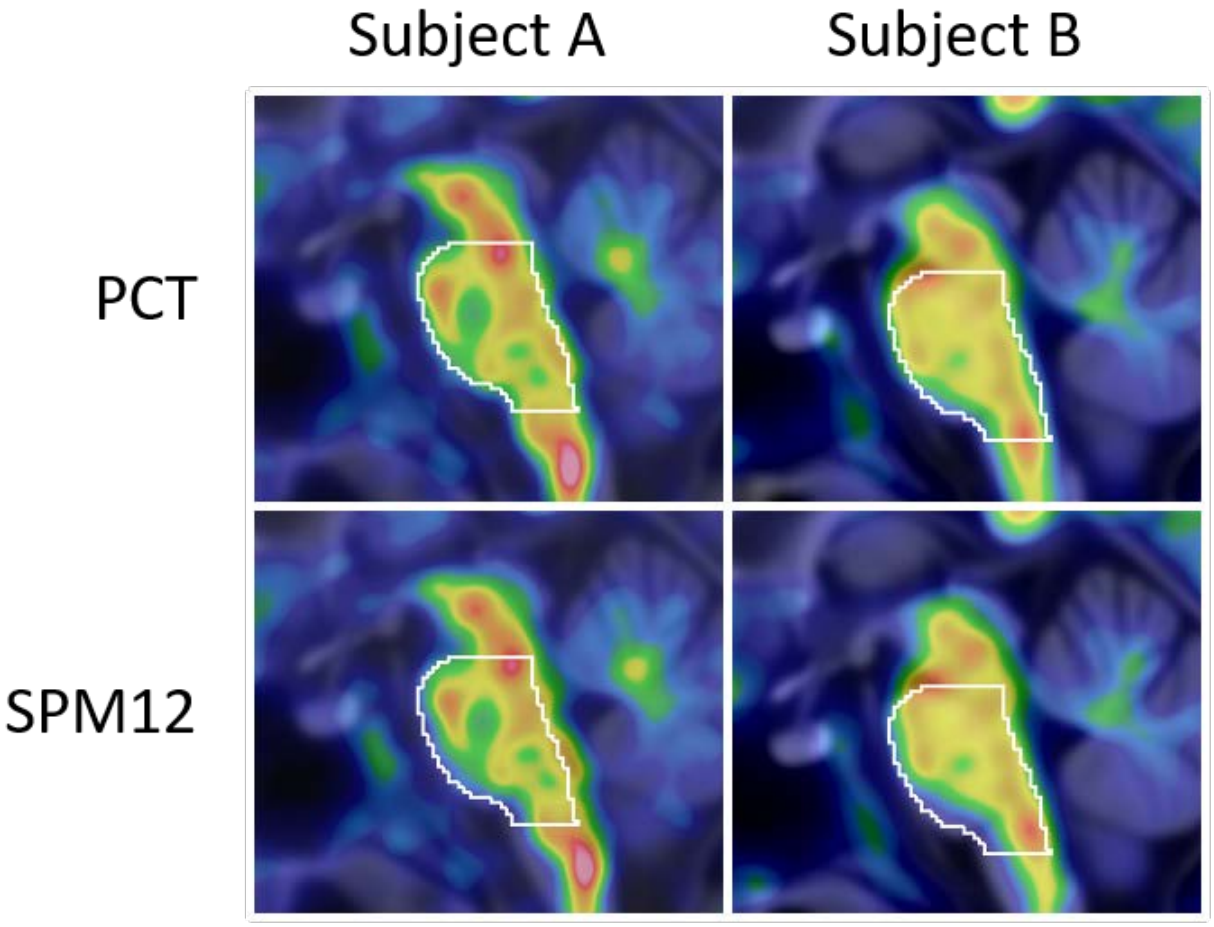

Supplemental Fig. 4. Validation Cohort: two subjects, A and B, show a better fit of the high uptake in Pons using principal component template registration than for the SPM registration.